FIBER-FED LASER-HEATED PROCESS FOR PRINTING TRANSPARENT GLASS

John M. Hostetler [i], Jonathan T. Goldstein [ii], Douglas Bristow [i], Robert Landers [i], Edward C. Kinzel [i]

[i] Department of Mechanical and Aerospace Engineering, Missouri University of Science and Technology, Rolla, MO
[ii] Air Force Research Laboratory, Materials and Manufacturing Directorate, Wright-Patterson Air-Force Base, OH

Abstract

This paper presents the Additive Manufacturing (AM) of glass using a fiber-fed process. Glass fiber with a diameter of 100 μm is fed into a laser generated melt pool. A CO_2 laser beam is focused on the intersection between the fiber and the work piece which is positioned on a four-axis computer controlled stage. The laser energy at λ=10.6 μm is directly absorbed by the silica and locally heats the glass above the working point. By carefully controlling the laser power, scan speed, and feed rate, bubble free shapes can be deposited including trusses and basic lenses. Issues unique to the process are discussed, including the thermal breakdown of the glass, buckling of the fiber against an inadequately heated stiff molten region, and dimensional control when depositing viscous material.

Introduction

Additive manufacturing has revolutionized the field of manufacturing in recent years due to the advantages that these processes entail. Traditionally these advantages have pertained to an increased design freedom and the allowance of complicated three-dimensional geometries, rapid prototyping, more efficient material usage, and the capability to manufacture parts from functionally graded materials. As these techniques for additive manufacturing mature however, more manufacturing applications become candidates for adaption to these processes. Specifically, applications for optical systems are emerging as a promising enterprise; applications such as photonics packaging, gradient index (GRIN) and freeform optics, and integrated optics all stand to benefit from the development of a system which is capable of depositing high quality optical materials. This is due in part to the attractive material properties of glass itself. Glass is transparent in the visible spectrum, is amorphous and therefore does not suffer from grain boundary scattering, it is chemically inert, harder than transparent polymer counterparts, and displays a low sensitivity to temperature gradients.

While additive manufacturing has been widely studied for use with polymers, metals and ceramics, there is comparatively little work done in developing AM techniques for glass[1]. Those studies which have been conducted into the AM of glass share a limitation in depositing transparent glass due to bubble entrapment. Several groups utilizing selective laser sintering were able to fabricate three-dimensional glass parts[2,3,4], but these parts resemble sugar cubes in both texture and appearance. The development of continuous melting approaches for glass AM

by several groups has been much more successful in depositing transparent glass. A filament-fed laser-heated process developed by Luo et al. demonstrated an ability to deposit void-free transparent glass using a feedstock with diameters ranging from 0.5-3 mm[5]. However, this process requires new cane to be reloaded into the filament feeder intermittently during the deposition process, and even the smallest diameter feedstock used of 0.5 mm cannot be rolled to extend the duration of uninterrupted deposition. Subsequently, Klein et al. developed a gravity-fed molten vat approach[6] and Micron3dp introduced their high temperature extrusion technique[7]. Both of these platforms are capable of depositing very intricate three-dimensional geometries out of glass, but the inability of these techniques to deposit void-free blocks of glass constrains their use for optical applications.

In light of the limitations with the filament-fed laser-heated process[5], a system utilizing optical fiber as a feedstock is very attractive, as kilometers of fiber may be spooled to allow for a continuous deposition process. In addition, the smaller diameter of optical fiber minimizes issues with thermal diffusion in the feedstock, potentially allowing for a greater volumetric deposition rate than that of the filament-fed process. Optical fibers are widely available, consisting of extremely high quality, low loss glass (<1 dB/km), and are relatively cheap with prices lower than $180 per km of single mode fiber[8].

Experiential Results

The experimental platform used in this study (Fig. 1) utilizes a CW CO_2 laser (Synrad Evolution 125, λ_0=10.6 µm, 140 µm spot size) which is incident on a soda-lime substrate. The substrate is fixed to a heater capable of reaching temperatures of 650℃, which is utilized to prevent thermal shock during the deposition process. The heater and substrate are in turn attached to a set of *x*-*y*-*z* stages, where the *x* and *y* stages (Aerotech ANT130-160XY) realize the horizontal movements, and a *z* stage (Aerotech ATS100-150) is used to move the platform upwards and downwards. A rotational stage (Aerotech ANT130-360-R) was installed on top of the *x*-*y*-*z* stages to enable rotations of the substrate. The fiber was fed into the melt pool (intersection of laser beam and substrate) by a custom-designed fiber feeder. 1% of the laser energy is reflected into a thermopile type power meter (Ophir 10A-V1) so that the laser power at the printing surface may be determined.

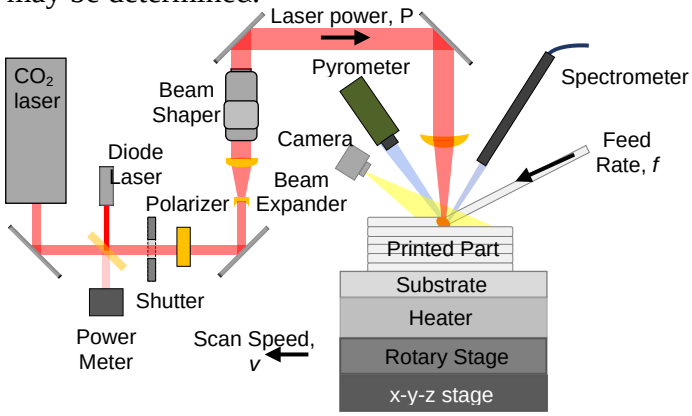

Fig. 1. Schematic of experimental platform

Incandescent light is emitted from the melt pool during the printing process, with the spectrum of the radiation being dependent on the temperature of the melted glass. This incandescent emission is collected using an OceanOptics USB-4000 fiber-coupled spectrometer (calibrated with an OceanOptics LS-1-CA 2800 K light source) which has a 0.8 mm diameter interrogation region centered on the laser heated area. The process parameters investigated in this study for their effect on the deposited glass are specified to be the laser power, *P*, fiber feed rate, *f*, and the platform scan speed, *v* (Fig. 2). The latter two parameters were consolidated into a dimensionless ratio of feed rate to scan speed, *f*/*v*.

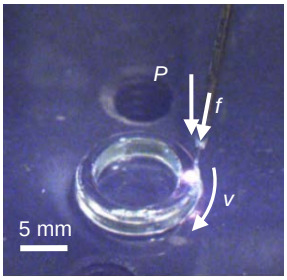

Fig. 2. Process parameters for fiber-printing specified for their effect on the deposited glass

The fiber used in this study was 100 µm soda-lime fiber provided by Schott. One of the challenges in working with this fiber involves the necessity to remove the encapsulating sizing on the fiber intended to prevent the fiber from fracturing at microcracks. Fiber stripping tools are widely available commercially, but these tools are typically only used to remove sizing on small strips of fiber, and when it is attempted to strip the fiber continuously, these mechanical methods result in the accumulation of residual sizing particulate on the fiber itself which burn off and deposit soot, thus limiting the transmissivity of deposited glass. Dissolving the sizing by soaking the fiber in ethanol for approximately thirty minutes prior to deposition proved to be a much more efficient approach, with initial transmissivity measurements finding that the transmissivity of the deposited fiber increased from 0.54 for untreated fiber to 0.79 after an ethanol bath.

Another significant challenge in developing a fiber-fed process is the act of feeding compliant fiber into a viscoelastic molten region. This requires a fiber feeder capable of addressing both fiber deflection and fiber buckling. To prohibit the fiber from deflecting out of the melt pool, a series of nested hypodermic tubes were used to guide the fiber from the feed wheels to the deposition site. (Fig. 3). The inner diameter of this tubing was chosen to be 140 µm to limit the friction between the fiber and the inner walls of the tubing.

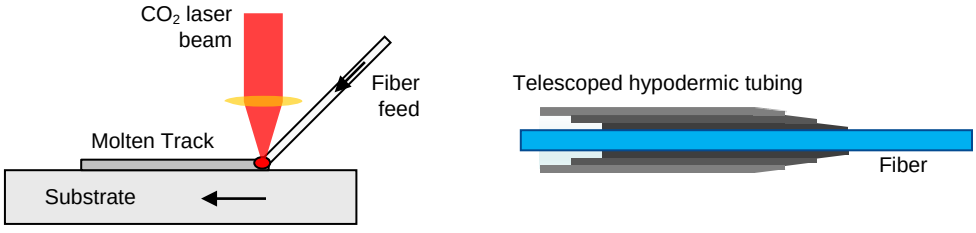

Fig. 3. Schematic of telescoping hypodermic tubing used to prohibit fiber deflection

The issue of fiber buckling continued to manifest in the unsupported span between the point of contact of the feed wheels and the entrance to the hypodermic assembly, labeled ‘d’ in Fig. 4. Here the fiber would buckle to such an extent as to cause it to snap, resulting in a deposition failure. It was found that this span, *d*, must be no greater than 2.4 mm in order to prevent the fiber from buckling. With these issues addressed, a continuous fiber deposition was enabled.

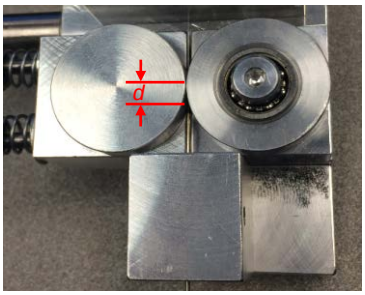

Fig. 4. Fiber feeder with span, *d*, identified as critical parameter to prevent fiber buckling

The process parameters *P* and *f*/*v* were first studied to identify their effects on the morphology of single tracks. Single tracks were deposited therefore over a range of parametric combinations of *P* and *f*/*v*, after which these tracks were cut and their cross sections polished. The track dimensions of height, h, width, w, and contact angle, θ, were then measured from these polished cross sections (Fig. 5).

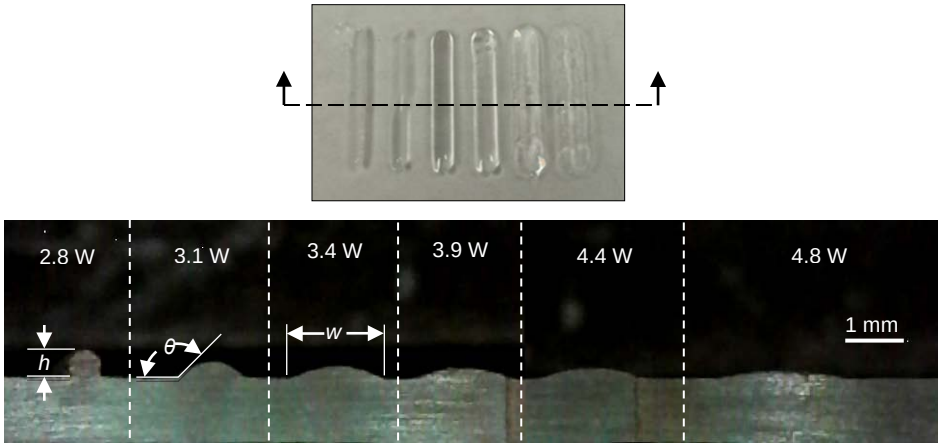

Fig. 5. Cross section of single tracks with measured dimensions labeled

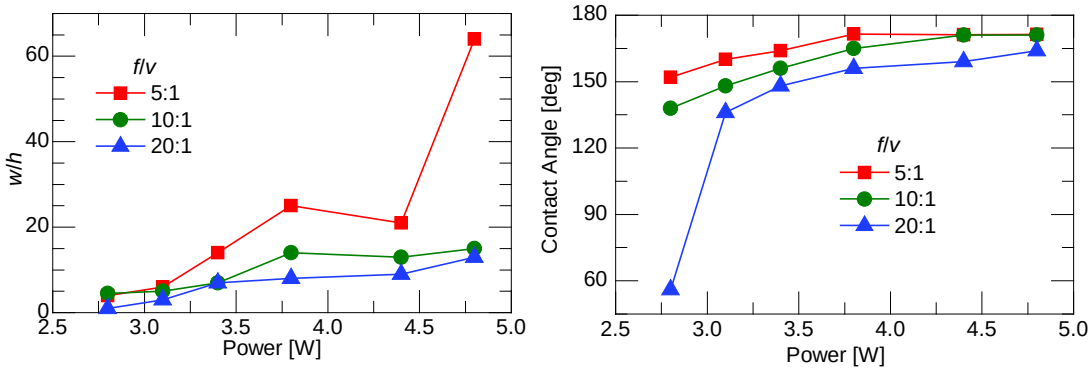

Fig. 6. Recorded dimensions of single track morphology as a function of process parameters

The dimensions recorded of single track morphologies (Fig. 6) were then utilized to determine appropriate step sizes for depositing 2D walls, consisting of several stacked single tracks. These walls were deposited at representative parametric combinations of *f/v* and *P*. After deposition, these walls were polished on both sides to create transmissivity samples (Fig. 7).

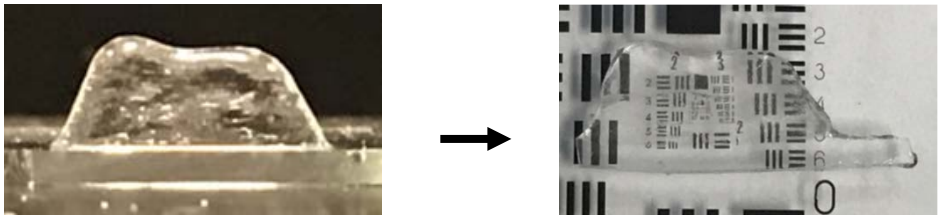

Fig. 7. 2D wall post-deposition (left), after polishing to create transmissivity sample (right)

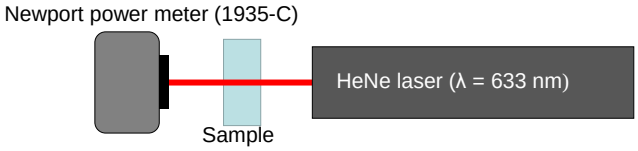

Fig. 8. Schematic of transmissivity measurement setup

The transmissivity of these polished samples were measured at a wavelength λ = 632.8 nm with a HeNe laser and a Newport power meter (1935-C). This was done by measuring the power of the HeNe laser beam unobstructed, then re-measuring the power of the beam after it is transmitted through a sample. It was found that the transmissivity trend of the deposited fiber was parabolic (Fig. 9). At lower laser powers, the fiber is softened and coils along the track, scattering any incident light and subsequently lowering the deposited part's transmissivity. At excessive laser powers, the soda-lime breaks down and is vaporized, depositing soot on the part which also lowers transmissivity. Between these two extreme cases however, a maximum transmissivity of 0.92 is measured for *f/v* = 15 and *P* = 6 W. This transmissivity value is ~93% of the transmissivity of conventionally manufactured soda-lime glass[9].

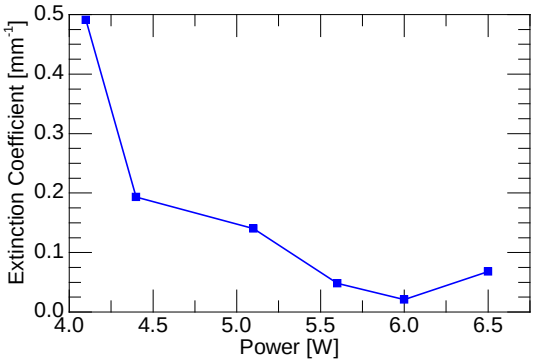

Fig. 9. Measured extinction coefficient of deposited fiber versus laser power

After determining the process parameters which result in the maximum transmissivity of the deposited soda-lime fiber, it was then attempted to deposit a simple lens with the fiber (Fig.

10). The lens was printed in a single continuous spiral deposition from the center outwards, with a constant f/v to create a convex profile.

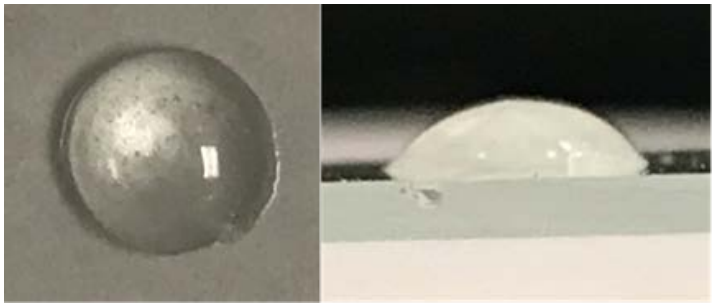

Fig. 10. Simple lens printed with soda-lime fiber post-deposition: top view (left), side view (right)

A large spot size (3 mm diameter) was used to reflow rings of the spiral during the deposition process to smoothen the lens surface; this reflow process however demonstrated a propensity for entrapping bubbles within the lens. Never the less, these simple printed lenses demonstrate the ability to optically focus light (Fig. 11).

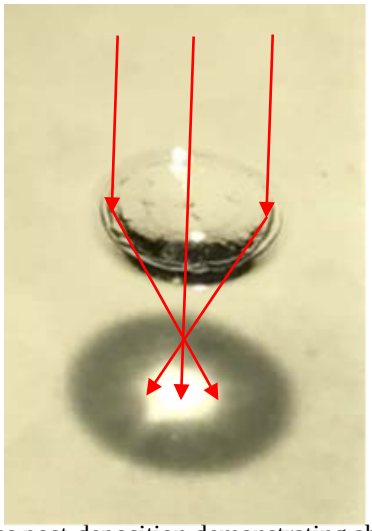

Fig. 11. Printed lens post-deposition demonstrating ability to focus light

In addition to depositing lenses, the fiber-fed laser-melted process has been found to be capable of depositing complex free-standing 3D structures, such as the spiral shown in Fig. 12. These types of deposition are enabled by the temperature-dependent viscosity of soda-lime glass. As the deposited fiber is moved away from the melt pool, it cools and the viscosity quickly increases, resulting in the structure becoming very rigid. There are several conditions however which must be maintained to ensure a successful deposition: In order to prevent the failure mode of ‘remelt’, wherein the laser softens a previously deposited structure causing it to collapse, the melt pool must be located at the focal point of the laser. In addition, an appropriate laser power must be used to ensure that the laser energy is completely absorbed by the melting fiber, and not allowed to continue beyond the deposition site and subsequently soften any preexisting structures beneath.

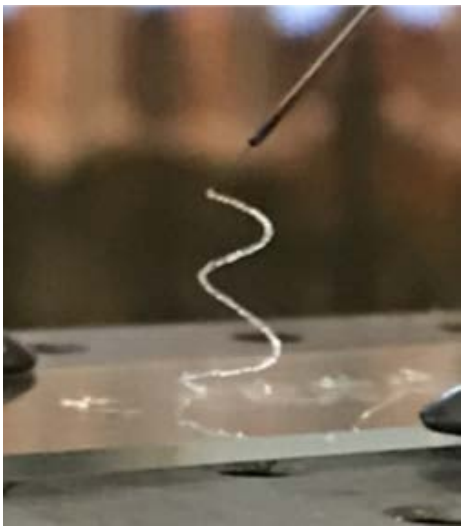

Fig. 12. Free-standing spiral deposited with fiber-fed process

Conclusions

A fiber-fed laser-heated process is capable of depositing soda-lime glass parts with a 100 µm fiber feedstock. Before deposition, an encapsulating sizing on the fiber must be removed via a thirty minute soak in ethanol. Telescoping hypodermic tubes successfully prevent the fiber from being deflected out of the melt pool, and the unsupported span between the entrance of these hypodermic tubes and the point of contact between the feed wheels must be less than 2.4 mm to prohibit fiber buckling. The fiber-fed process deposits glass with a maximum transmissivity of 0.92 (93% of the transmissivity of conventionally manufactured soda-lime glass) with the parameters f/v = 15 and P = 6 W. The process has demonstrated an ability to deposit simple lenses capable of focusing light, as well as depositing complex free-standing three-dimensional structures.

Acknowledgements

This work was supported by the National Science Foundation (CMMI-1538464) as well as the Air Force Research Laboratory.

References

[1] G. Marchelli, R. Prabhakar, D. Storti, M. Gantor, “The guide to glass 3D printing: developments, methods, diagnostics and results”, *Rapid Prototyping Journal* **17**(3), 187-194 (2011).

[2] R. Khmyrov, S. Grigoriev, A. Okunkova, and A. Gusarov, "On the Possibility of Selective Laser Melting of Quartz Glass" *Physics Procedia* **56**, 345-356 (2014).

[3] J. Hostetler et al., “Selective Laser Sintering of Low Density, Low Coefficient of Thermal Expansion Silica Parts”, *Proceedings of Solid Freeform Fabrication Symposium. Austin, TX*, 978-988 (2016).

[4] M. Fateri, A. Gebhardt, “Selective Laser Melting of Soda-Lime Glass Powder” *Int. J. Appl. Ceram. Technol.*, **12**(1) 53-61 (2015).
[5] J. Luo, H. Pan, E. Kinzel, “Additive Manufacturing of Glass”, *J. Of Mfg. Sci. and Eng.*, **136**, 061024-1 (2014).
[6] J. Klein, M. Stern, G. Franchin, M. Kayser, C. Inamura, S. Dave, J.C. Weaver, P. Houk, P. Colombo, M. Yang, “Additive manufacturing of optically transparent glass,” *3D Printing and Additive Manufacturing*, **2**(3), 92-105, 2015,
[7] http://micron3dp.com/blogs/news/34473924-breakthrough-in-3d-printing-glass (2015)
[8] https://www.corning.com/media/worldwide/coc/documents/Fiber/SMF-28%20Ultra.pdf
[9] https://refractiveindex.info/?shelf=glass&book=soda-lime&page=Rubin-clear